A COMPACT, PORTABLE WET PAINT THERMAL WAVE THICKNESS MONITOR

Jeffrey P SARGENT and Simon CHURCH

Advanced Technology Centre, BAE SYSTEMS, Bristol, BS34 7QW, UK

Abstract

The design, construction and testing of a non-contact, non-destructive, compact, thermal wave coating thickness measurement system is described. The system is based on heating the surface using a semiconducting laser and measuring the resulting thermal wave phase at the surface using a pyroelectric sensor. Measurements are described for coatings and free films using epoxy primer and metal loaded paint films. Analysis is presented which gives the thermal wave phase relationship for free, unsupported films in transmission. A methodology is described for making measurements of wet paint film thickness, from which the dried and cured paint film thickness may be inferred. A portable, compact thermal wave system has also been designed and constructed which would permit implementation of this method.

Introduction

The precise control of paint film thickness is important for aircraft in order to control their weight. Of particular interest to the study reported here was the non-destructive measurement of wet paint film thickness, rather than dry paint film thickness. This distinction between measurements on wet paint, as opposed to dry paint, arose, because in order to give a final dry paint film with the necessary thickness, it is necessary to control spraying parameters in real time and measure paint thickness as the wet paint is applied, and before the paint dries. To accomplish this, the method used must be both non-contact and rapid, and there must also be an understanding of the relationship between the measured wet paint film thickness and the final thickness after the paint has dried.

The principles of thermal wave film thickness measurement is based on the established methodology for dry films and coatings, whereby photothermic measurements of phase at the coating surface can be related to layer thickness via an analysis of the thermal wave propagation within the layer as given by, for example, Almond (1). The technique is non-contact and is potentially fast and accurate. The method works analogously to the use of ultrasound methods, except that layer thickness is deduced from the transit time of thermal waves if the thermal diffusivity is known. Commonly, when used with periodic-harmonic excitation, the transit time is derived from phase measurements of surface temperature with respect to the phase of the excitation source.

An initial evaluation of the procedure necessary to undertake a dry paint thickness measurement from a wet paint thickness measurement was first made by using a laboratory based system, in which the thermal wave phase/thickness relationship was established between the wet paint and the final dry and cured paint. Having once established a methodology and procedure, the design, construction and validation of a portable thermal wave system is also described by reference to measurements of various dry films on different substrates. In addition, analysis and measurements are also presented for measuring the thickness of free, unsupported films.

Experimental method

Both the laboratory based and compact portable system used the same principle of photothermic generation and detection of thermal wave. The laboratory system will be described first.

1) Laboratory based thermal wave system

Initial test of the viability of wet paint thickness measurements were made using an argon/ion based laser system. This was a coherent beam 3W argon ion laser with a wavelength of 514nm. Briefly, laser light was mechanically chopped to generate a periodically fluctuating surface temperature within a frequency range of between 10Hz and 34Hz. A specimen was mounted on a translation stage and amplitude and phase of the temperature under the illuminated spot was monitored via a Mullard 825CPY triglycine sulphate pyroelectric detector placed at the focus of an ellipsoidal mirror. The specimen dwelled for a short time (typically between 1 and 3 seconds), and the phase was measured with reference to the illumination via a phase-locked loop amplifier (using an integration time typically between 0.1 and 3 seconds) and recorded on a PC.

2) Compact portable thermal wave system

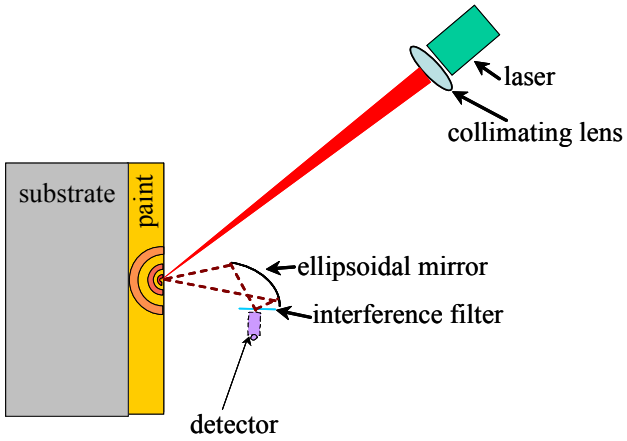

Figure 1. Schematic diagram showing the optical elements of the compact portable thermal wave system.

The essential optical elements of the compact thermal wave paint thickness measurement system are shown schematically in Figure 1. The system comprised a 1 watt CW infra-red (809nm) semiconductor laser diode (High Power Devices, HPD1010-T03-80803) housed in a medium power laser diode heat sink mount. The laser was driven by a dedicated low noise laser diode driver current source with external analogue modulation input control (Model 525AN, Newport). Short wavelength infra-red radiation from the laser diode was collimated via an aspherical lens with focal length 6.24mm, and focussed onto the paint film on the test piece giving a heated area of a few mm in diameter. Modulation of the laser driver current source was via the reference channel of the lock-in amplifier, giving a linear optical laser power output of between ~0W and ~0.3W. Long wavelength infra-red radiation emitted from the test piece as a result of heating was focussed via a front surface, gold coated, off-axis ellipsoidal mirror (D=42mm, F1=25mm, F2=80mm, Interspectrum OU). After focussing, the long wavelength infra-red radiation passed through an interference filter (reflectance of >95% at 809nm, transmission >93% at 10μm, Reynard Corporation) onto a germanium windowed pyroelectric detector with integral JFET pre-amplifier (thermal time constant 18ms, DLATGS Type No P5368, BAE Systems Infra-red Ltd). The detector was biased in a source follower configuration

with a load resistance of 56K ohms using the circuit shown in Figure 2. This in turn gave a photodetector output of sufficient magnitude to permit phase measurements at frequencies in the range of between approximately 0.15Hz and 60Hz. Output and recovered signal phase from the load resistor was then detected using a lock-in amplifier (METEK, DSP Model 7265) which was measured with respect to the internal reference modulation frequency generated by the lock-in amplifier. The quality of the waveform was also routinely monitored with an oscilloscope. Initial mounting and alignment was first performed on an optical table, this also permitted the opportunity to conduct some measurements in transmission, as well as in reflection. Once aligned, the reflection system was mounted in a small dedicated box with dimensions of 25cms x 25cms x 10cms, with an exit hole at the focus of the ellipsoidal mirror and collimating lens, with all cable lead throughs located at the rear of the box. Figure 3 shows the optical components mounted in the box both with and without the lid in place.

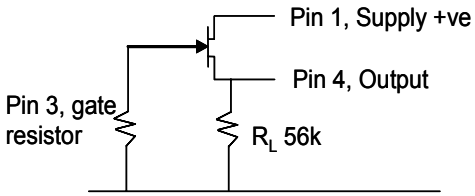

Figure 2. Circuit diagram for biasing the photodetector.

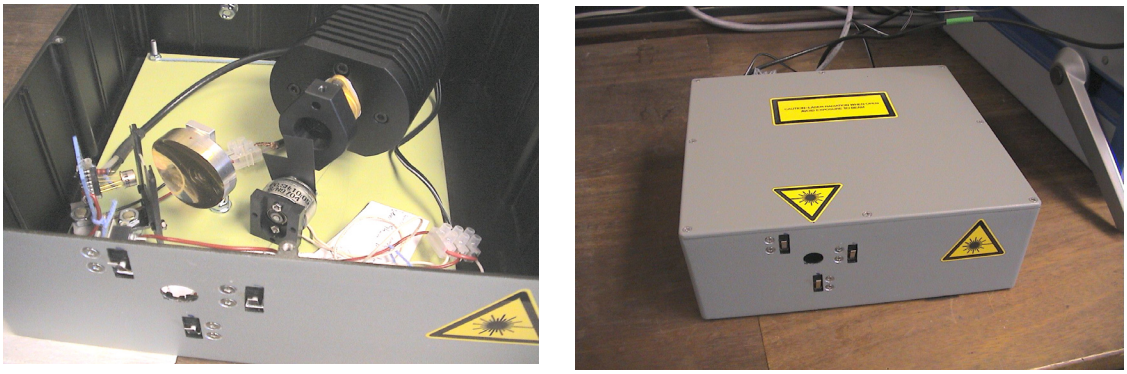

Figure 3. The compact thermal wave system, with (left) the optical components visible and (right) with the lid in place.

3) Methodology

Initial testing was first conducted on primer painted aluminium substrate panels using the laboratory based thermal wave system. This was undertaken in order to measure the thermal properties of the cured paint. Corroborative measurements of thickness on the dry paint specimens was undertaken using an eddy current thickness tester (DeFelsko Positector® 6000), and a differential focussing arrangement on an optical microscope (Zeiss Axioplan®) using a large magnification objective lens with a small depth of field. This was undertaken by removing a small region of paint such that the substrate was exposed, and then focussing in turn on the paint surface and the paint/aluminium interface, and then noting the traverse of the stage required for focussing. Initial characterisation and measurement of wet paint thickness changes as the paint dried were made on specimens painted to a known thickness using draw bars. Thickness measurements for these specimens were made using the laboratory thermal wave system and the differential focussing arrangement on the optical

microscope. These were made as a function of time. Subsequent tests on dry paint comprising primer and metal loaded paints on aluminium and CFRP substrates, and for free unsupported films were undertaken using the compact portable system.

Thermal wave analysis

Case 1: Reflection mode, no absorption of incident laser radiation in film

Almond (1) gives the relationship between phase (phase20(L)) and paint film thickness (L) on a substrate at a given modulation frequency (ω) as:

$$\text{phase20(L)} := \operatorname{atan}\left[-1 \cdot \frac{(1 + \text{Rbg}) \cdot \text{Rbb} \cdot e^{-\text{x20(L)}} \cdot \sin(\text{x20(L)})}{1 + \left[(1 - \text{Rbg}) \cdot \text{Rbb} \cdot e^{-\text{x20(L)}} \cdot \cos(\text{x20(L)}) \right] - \text{Rbb}^2 \cdot \text{Rbg} \cdot e^{-2 \cdot \text{x20(L)}}} \right] \qquad (1)$$

where: L = thickness
Rbg = thermal reflection coefficient at air/paint interface
Rbb = thermal reflection coefficient at substrate/paint interface
x20 = $2L/\mu$
μ = $(2\alpha/\omega)0.5$
α = thermal diffusivity

Case 2: Reflection mode, absorption of incident laser radiation in film,

Case 3: Reflection mode, no absorption of incident laser radiation in film, but thermal contact resistance between paint film and substrate

It should be noted that equation 1 is valid for heat generation at the surface of the paint film, and is appropriate for visible incident laser radiation, where the absorption depth is small and heating is confined to the paint surface. However with longer wavelength radiation, such as the longer wavelength 809nm laser radiation from the semiconductor laser used here, heating may not be confined to the surface, but may instead occur within the bulk of the paint film. In this instance it then necessary to use the appropriate models with the correct heat distribution. A further case can also be identified where, although heating is confined to the surface layer, the presence of thermal contact resistance between paint film and substrate results in an additional modification to the analysis. Both the instance of bulk absorption (Case 2) and thermal contact resistance (Case 3) have been theoretically described by Almond (1) in terms of the complex surface temperature. Both of these cases have been used here in order to correlate measurements with theory.

Case 4: Transmission mode, no absorption of incident laser radiation in film.

In some instances, it is also useful to have a non-contact transmission measurement thickness of a free unsupported film, where heating is from one side and phase is measured from the opposite side of the film. In this case, the analysis, which has been developed here, is where the heating is confined to the surface and bulk absorption is not present. By heating at the front paint surface and by consideration of the propagation of thermal waves incident at both the front air/paint and rear paint/air interface the complex surface temperature (Film20(L)) at the rear of the paint film can be shown to be:

$$\text{Film20}(L) := 1 \cdot \text{Tbg} \cdot \frac{(1 + \text{Rbg}) \cdot \exp(-\sigma\text{paint20} \cdot L)}{1 - \text{Rbg}^2 \cdot \exp(-2 \cdot \sigma\text{paint20} \cdot L)} \qquad (3)$$

An explicit derivation for the phase (phaseT20(L)) may then be derived after some algebraic manipulation:

$$\text{phaseT20}(L) := \frac{360}{2 \cdot \pi} \cdot \text{atan}\left[-1 \cdot \frac{1 \cdot \sin\left(\frac{x20(L)}{2}\right) + \text{Rbg}^2 \cdot \exp(-x20(L)) \cdot \left(\sin(x20(L)) \cdot \cos\left(\frac{-x20(L)}{2}\right) - \cos(-x20(L)) \cdot \sin\left(\frac{x20(L)}{2}\right) \right)}{1 \cdot \cos\left(\frac{x20(L)}{2}\right) - \text{Rbg}^2 \cdot \exp(-x20(L)) \cdot \left(\sin(x20(L)) \cdot \sin\left(\frac{x20(L)}{2}\right) + \cos(-x20(L)) \cdot \cos\left(\frac{-x20(L)}{2}\right) \right)} \right] \qquad (4)$$

Results

1) Dry paint in reflection

a) Primer paint

Fig. 4a shows the results of a best fit for equation 1 to the average measured thickness for a series of primer paint layers on aluminium substrate specimens using the laboratory system at 10Hz, 20Hz and 30Hz. Using quoted values for the density and thermal properties of aluminium [1], together with a quoted paint density $\rho = 1620 kgm^3$ [2] and an estimate for the paint specific heat $c_p = 1300 Jkg^{-1}K^{-1}$ yielded a single value for the paint thermal conductivity $k = 0.55\ Wm^{-1}K^{-1}$ and a thermal diffusivity $\alpha = 2.6 \times 10^{-7}\ m^2s^{-1}$ from the fitting procedure. These values are collated in Table 1. Figure 4b shows results obtained using the compact portable system using the same primer paint and aluminium thermal properties as given in Table 1 over an extended frequency range and primer paint thickness range. In this instance, the theoretical curves are based on the analysis given in Case 2 above, with a skin depth of 11μm. A good fit is evident for both the laboratory and compact thermal wave system at all frequencies and for all thicknesses.

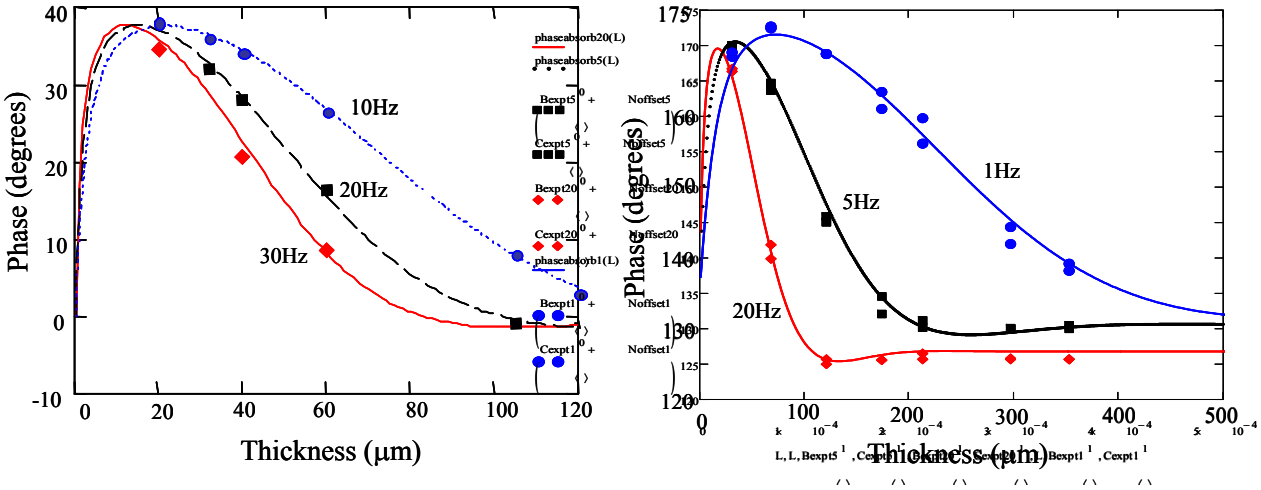

Figure 4a (left), Experimental results and theoretical curves (Case 1) for primer painted aluminium specimens using the laboratory system, b (right), Experimental results and theoretical curves (Case 2) for primer painted aluminium specimens using the compact system.

Material	Density Kgm^{-3}	Specific heat $Jkg^{-1}K^{-1}$	Diffusivity $x10^{-6}m^2s^{-1}$	Conductivity $Wm^{-1}K^{-1}$
Aluminium	2700	945	93	238
CFRP	1420	1130	$1.3x10^{-6}$	2.8
Primer paint	1620	1300	$2.6x10^{-7}$	0.55
metal loaded primer, low Vf	2800	1087	$2.14x10^{-7}$	0.65
metal loaded primer, high Vf	4420	874	$3.9x10^{-7}$	1.5

Table 1. Thermal properties of dry paints and substrates used in this study

b) High volume fraction metal loaded paint

Paint films comprising metal loaded primer paint on aluminium and CFRP substrates with a high volume fraction were measured using the compact thermal wave system. It was noticeable that the paint was poorly bonded to both substrates, and it was necessary to incorporate a thermal contact resistance in the analysis (Case 3) between substrate and paint layer. Theoretical predictions for the paint were based on the thermal properties given in Table 1, with a thermal conductivity of 1.5 W m^{-1} K^{-1}, a density of 4420kg/m^3, and a specific heat of 874J kg^{-1} K^{-1} derived using a rule of mixtures approximation based on the specific heat of the two paint components. Figure 5a shows results and theoretical curves for the aluminium substrate using 0.5Hz and a thermal contact resistance of 0.00004, and Figure 5b for the CFRP substrate using 0.15Hz and thermal contact resistance of 0.00007. Agreement was again good between experimental results and theory.

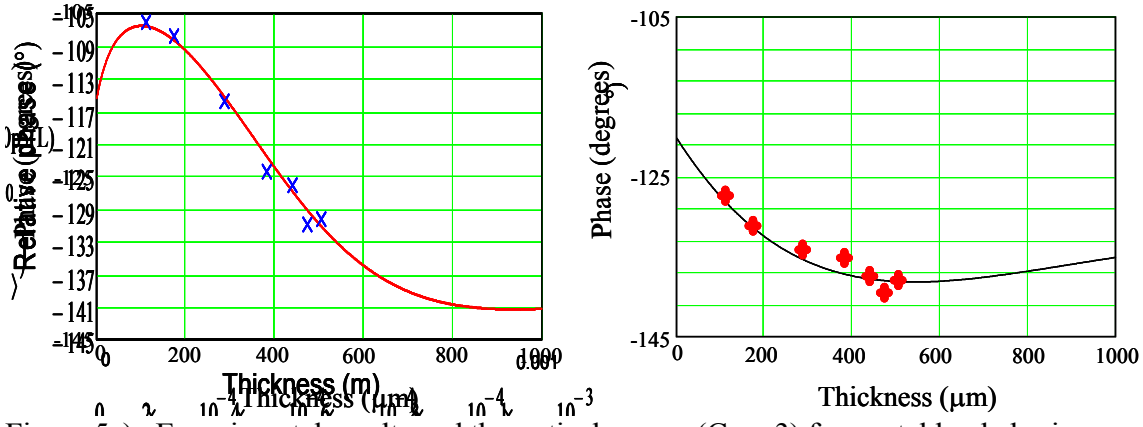

Figure 5a), Experimental results and theoretical curves (Case 3) for metal loaded primer painted on aluminium specimens (left) at 0.5Hz, and b) (right) for metal loaded primer painted on CFRP specimens at 0.15Hz.

2) Free film in transmission

Figure 6 shows phase/thickness results and transmission predictions using equation 4. These are for free unsupported specimens comprising a low volume fraction metal loaded paint with

thickness of 72µm, 77µm and 85µm. Predictions for the low volume fraction film were based on the thermal properties given in Table 1, with paint properties again derived using a rule of mixtures based on the specific heat of the individual paint components as described previously. Good agreement between theory and experimental results over this restricted range of thickness was evident.

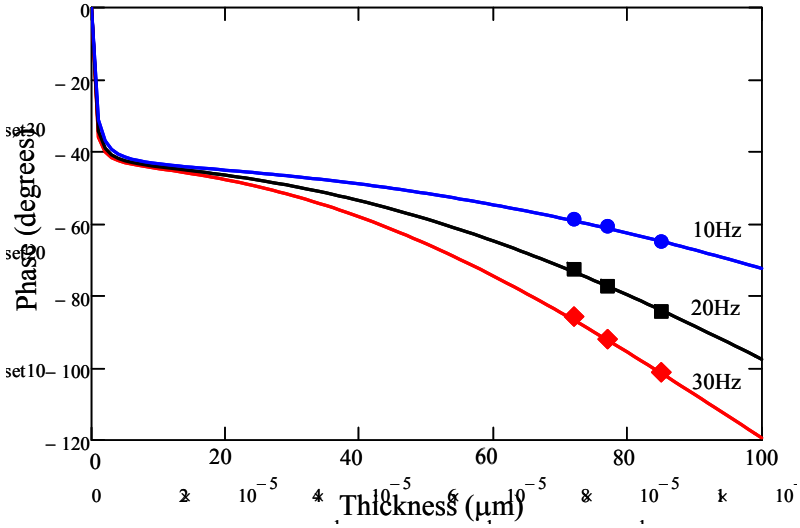

Figure 6. Predicted phase/thickness relationships derived using equation 4 for transmission through unsupported low volume fraction metal loaded paint. Also shown are experimental results at 10Hz, 20Hz and 30Hz obtained using the laboratory based compact thermal wave paint thickness monitor.

3) Wet paint in reflection

Employing a differential optical thickness measurement technique described previously, an example of the change in thickness of an applied primer paint films as it dried is shown in Figure 7. Noting that the drying is primarily controlled by the release of solvent from the paint, a reasonable approximation to this initial drying phase is to model the diffusion within the paint and fit a functional form based on this process.
By assuming that the wet thickness of a paint film containing a fractional content of solvent at time t may be related to the dry thickness (h_0) via an initial solvent fraction at time t =0 (C_0) and a fractional mass loss at time t ($M_{fract(t)}$), then the thickness h(t) at time t may be written as:

$$h(t) = C_0 \,.\, M_{frac(t)} \,.\, h_0 + h_0 \qquad (5)$$

where: $M_{frac(t)} = M_t/M_\infty$

Noting that Crank [3] gives an error function (erfc) solution for sorption and desorption from a membrane in terms of the ratio between the mass of diffusing substance at time t (M_t) and at time t = ∞ (M_∞), then the fractional mass loss from a thin film ($M_{frac(t)}$) due to diffusion is:

$$M_{fract(t)} := 1 - 2\cdot\sqrt{\frac{D\cdot t}{L^2}}\cdot\left[\frac{1}{\sqrt{\pi}} + 2\cdot\sum_{n=1}^{\infty}\left[(-1)^n\cdot ierfc\left(\frac{n\cdot L}{\sqrt{D\cdot t}}\right)\right]\right] \qquad (6)$$

where: D = diffusion coefficient
L = thickness of film

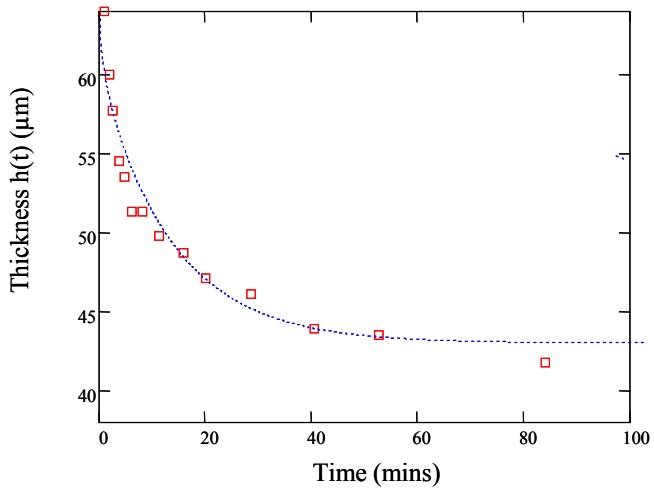

Figure 7. Drying curve for a 40µm paint layer measured using optical microscope □. Predicted thickness using diffusion solution equations 5 and 6 (dashed line).

Figure 7 also shows an example of fitting a curve to the measured thickness changes based on equations 5 and 6 using a solvent diffusion coefficient (D) of 9 x 10^{-13} m^2 sec^{-1}. Based on the results from a total of four such drying curves, it was estimated that there was an average fractional change in thickness from the wet state at time = 0 to its eventual dry film thickness after solvent release of approximately 49±1.5 %.

A derivation of a dry and cured paint film thickness from a measurement of phase for the paint in its wet state at some time t_1 after paint application requires not only the shrinkage that occurs during drying, but also knowledge of the thermal conductivity, specific heat and density changes that also occur.

Since no thermal properties of the wet paint were available it was necessary to estimate their likely evolution as the paint dried and cured. This was undertaken by assuming similar changes would occur as observed by Wubbenhorst et. al [4] for the cure of a DGEBA epoxy system, who noted a ~40% rise in thermal effusivity (specific heat x density x thermal conductivity)$^{1/2}$ before vitrification, and ~20% fall during vitrification (i.e. between its dry and cured state). By also noting that the wet paint was likely to be composed of 49% solvent at the moment of application, then a rule of mixtures relationship was also applied to estimate the thermal properties assuming a time dependent solvent content as given by equation 6. This was based on the solvent MEK, which is a common solvent for paints, with density ρ = 804 kg m^{-3}, specific heat C_p = 2300 J $kg^{-1}K^{-1}$ [5] and thermal conductivity k = 0.15 W m^{-1} K^{-1} [6]. It was also assumed that the dry thickness was 5% thicker than the cured thickness.

Table 2 summarises the estimated cured, dry and wet paint properties. Fig. 8 (a), (b), (c) and (d) shows the phase/thickness relationship calculated using equation 1 based on the estimated paint properties from Table 2 and analysis described above. Fig. 8 also shows the experimental points measured for the wet paint at time t_1 using the laboratory system after a) 30- 40seconds, b) after approximately 1.5minutes, c) when dry after solvent evaporation, and d) when the paint was fully cured.

Except for three results at the largest thickness in the wet state at 30 – 40 seconds, agreement between experiment and predictions at each time is good. Inspection of the final paint surface showed evidence that paint slump had occurred for these three results, and it is believed this resulted in the poorer observed agreement at 30 - 40 seconds. Excluding these three results, it was estimated that a phase measurement on the wet paints after 30-40 seconds from application could be used to predict a final cured paint thickness with an accuracy of approximately ±2µm.

Paint state	density (ρ) kg m^{-3}	specific heat (C_p) J $kg^{-1}K^{-1}$	thermal conductivity (k) W m^{-1} K^{-1}
cured	1620	1300	0.55
dry	1543	1625	0.41
wet (49%MEK)	1296	1848	0.32

Table 2. Estimated density and thermal properties for CA7012 primer paint in its wet and dry state.

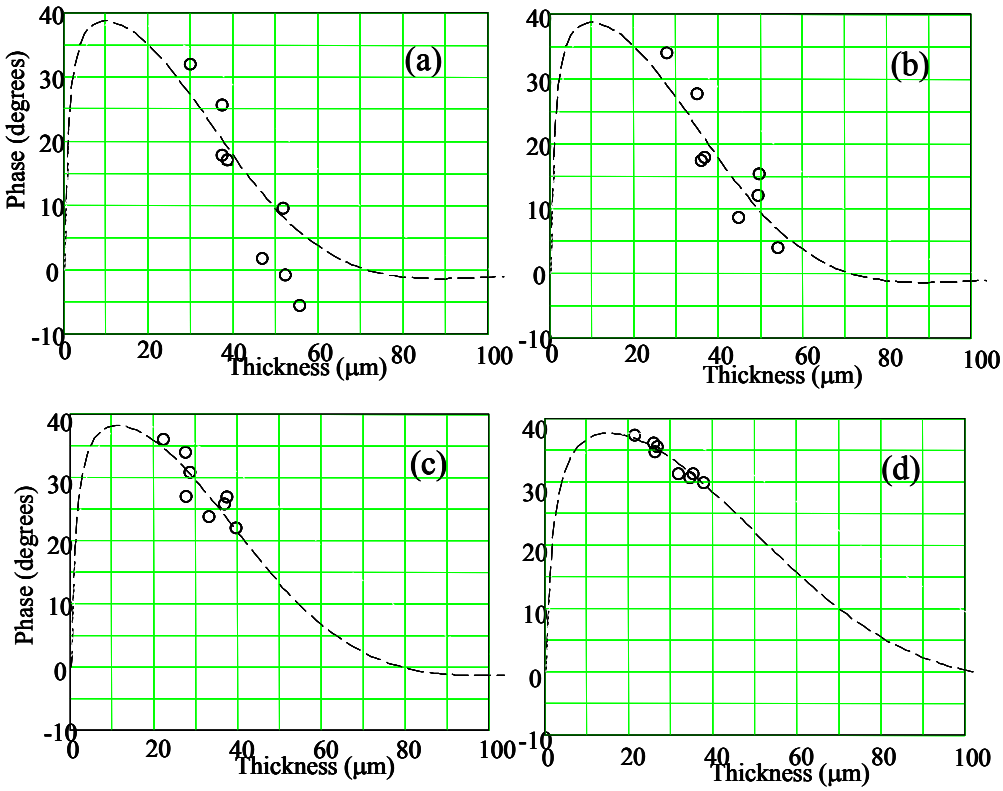

Figure 8. Sequence of phase/thickness predictions and measured thickness for the drying and curing of several painted specimens on aluminium substrates. Predictions based on thermal data from Table 2. a) Wet state, 40secs from time = 0, b) Results at ~1.5mins from time = 0, c) Results for dry state, d) Results after final cure.

Discussion

A prototype non-contact, compact, thermal wave paint film thickness measurement system has been designed and assembled which permits measurement of film thickness typically between ~10μm and ~ 1mm over a range of frequencies between 60Hz and 0.1Hz respectively. The accuracy with which a dry measurement of paint thickness was made was determined by a combination of the frequency range, the time constant employed in obtaining a phase measurement, the substrate type, the location on the phase/thickness graph of the measurement and the signal to noise ratio obtained from the detector. Thus, for example, an accuracy of approximately 0.5μm at 20Hz was obtained for a dry film thickness of ~50μm on an aluminium substrate using a time constant of 2 seconds, whereas the accuracy was much

reduced for paint films on CFRP substrates because the thermal properties of paint and substrate were similar.

When inferring cured paint film thickness from wet paint phase measurements additional errors are also introduced because of the assumptions used in the analysis. This includes the approximation of a fixed boundary diffusion solution for the evaporation of a known quantity of solvent from the paint, an approximation of the evolution of the paints thermal properties during drying based on a rule-of-mixtures analysis for paint and solvent, the application of literature values regarding changes in specific heat and thermal conductivity as the paint cured, and an assumed 5% change in thickness when the paint film cured. In addition, final accuracy was probably also determined by paint slumping.

For the paint films applied here using a draw bar method the solvent content and initial cure state of the wet paint were fairly well controlled. However when using paint which is sprayed from a spray gun, it is likely that care will have to be exercised over variables which influence paint spraying parameters which might influence evaporation of solvent from the paint, this includes spraying pressure, fan size, stand-off distance, gun speed, paint flow rate, etc. In addition, care would clearly also have to be given to controlling the residence time of paint which is held in a pot prior to painting, when any initial curing reactions will affect both the spraying process and the thermal properties of the paint. These will become increasingly important the longer the mixture is kept after addition of the accelerator.

In spite of these complications, a methodology has been demonstrated which would permit the derivation of cured and dried paint film thickness from thermal wave phase measurements conducted on a wet paint film. A compact portable unit has also been designed and made which, with some small additional modifications, could also be used for wet paint thickness measurements.
The comment should also be made that since it was necessary to include a thermal contact resistance for measurements with the metal loaded paints, which was with poorly adhered paint films, then such a measurement might be of use in future as a sensitive indicator of bond quality between the paint layer and the substrate.

Conclusions

Thermal wave phase measurements have the potential to form a relatively inexpensive means for a compact, light weight and quick method for making measurements of wet paint film thickness, from which the dried and cured paint film thickness may be inferred. This could be of significant benefit in paint spraying when accurate layer thickness is required, because it permits rapid feedback which may be used to control paint spraying parameters. A methodology has been demonstrated whereby this could be undertaken, and a portable, compact system designed and constructed which would permit implementation of this method. An analysis has also been presented whereby thermal measurements of phase may be use to make non-contact measurement of the thickness of free, unsupported films.

It is important, however, that if the technique is used for the application of paints to give a controlled paint thickness, then a critical awareness of the assumptions and approximation used in the analysis should be exercised. This would include the uncertainty of the initial known solvent content, uncertainty in the thermal properties of the paint during cure and drying, and also the extent of cure shrinkage on a final predicted thickness.

Acknowledgements

The authors would like to thank D P Almond and N Gathercole, University of Bath, UK, for help with making some of the laboratory based thermal wave measurements and also for advice on the construction of the compact portable thermal wave system. They would also like to thank T Campbell, BAE Systems, Military Air Solutions, UK.

References

[1] D P Almond and P M Patel, "Photothermal Science and Techniques", Chapman and Hall, 1996.

[2] Epoxy Primer CA7012 Technical Data Sheet 08/05/98, PRC DeSoto.

[3] J Crank, "The Mathematics of Diffusion", Oxford, 1964.

[4] M Wübbenhorst, J Van Turnhout and L Alili, Ferroelectrics, **165**, 153, 1995.

[5] "Product Description, Methyl Ethyl Ketone", PB-020-2 (May 2000), [Online]. Available from: http://www.tera.org/peer/VCCEP/MEK/Appendix%20D%20-%20MEK%20Product%20Brochure.pdf, [5 Nov 2009].

[6] "MatWeb.com, The Online Materials Database: Methyl Ethyl Ketone ($CH_3CH_2COCH_3$; 2-Butanone; MEK)", [Online]. Available from: http://www.matweb.com/search/SpecificMaterialPrint.asp?bassnum=VORG031, [5 Nov 2009].